



Published in final edited form as:

Glycoconj J. 2021 June ; 38(3): 347–359. doi:10.1007/s10719-020-09961-9.

Glycation-mediated protein crosslinking and stiffening in mouse lenses are inhibited by carboxitin *in vitro*

Sandip K. Nandi¹, Johanna Rankenberg¹, Stefan Rakete^{1,5}, Rooban B. Nahomi¹, Marcus A. Glomb², Mikhail D. Linetsky³, Ram H. Nagaraj^{1,4,*}

¹Sue Anschutz-Rodgers Eye Center and Department of Ophthalmology, School of Medicine, University of Colorado, Anschutz Medical Campus, Aurora, CO 80045;

²Institute of Chemistry-Food Chemistry, Martin-Luther-University Halle-Wittenberg, 06120 Halle/Saale, Germany;

³Department of Chemistry, Case Western Reserve University, Cleveland, OH, 44106;

⁴Department of Pharmaceutical Sciences, Skaggs School of Pharmacy and Pharmaceutical Sciences, University of Colorado, Anschutz Medical Campus, Aurora, CO 80045.

⁵Present address: Institute and Clinic for Occupational, Social and Environmental Medicine, University Hospital LMU Munich, Ziemssenstr. 1, D-80336 Munich, Germany

Abstract

Proteins in the eye lens have negligible turnover and therefore progressively accumulate chemical modifications during aging. Carbonyls and oxidative stresses, which are intricately linked to one another, predominantly drive such modifications. Oxidative stress leads to the loss of glutathione (GSH) and ascorbate degradation; this in turn leads to the formation of highly reactive dicarbonyl compounds that react with proteins to form advanced glycation end products (AGEs). The formation of AGEs leads to the crosslinking and aggregation of proteins contributing to lens aging and cataract formation. To inhibit AGE formation, we developed a disulfide compound linking GSH diester and mercaptoethylguanidine, and we named it carboxitin. Bovine lens organ cultured with carboxitin showed higher levels of GSH and mercaptoethylguanidine in the lens nucleus. Carboxitin inhibited erythrose-mediated mouse lens protein crosslinking, AGE formation and the formation of 3-deoxythreosone, a major ascorbate-derived AGE precursor in the human lens.

Terms of use and reuse: academic research for non-commercial purposes, see here for full terms. <http://www.springer.com/gb/open-access/authors-rights/aam-terms-v1>

*Correspondence should be addressed to: Ram H. Nagaraj, Ph.D., Department of Ophthalmology, University of Colorado, School of Medicine, 12800 East 19th Avenue, RC-1 North, 5102, Aurora, CO 80045. Phone: 303-724-5922. Fax: 303-724-5270. ram.nagaraj@cuanschutz.edu.

Author contributions

RHN and ML conceptualized the project. SKN, JR, SR and RBN conducted the experiments. SKN, SR, JR and RHN analyzed the results. All authors wrote the paper and approved the manuscript.

Publisher's Disclaimer: This Author Accepted Manuscript is a PDF file of a an unedited peer-reviewed manuscript that has been accepted for publication but has not been copyedited or corrected. The official version of record that is published in the journal is kept up to date and so may therefore differ from this version.

Conflicts of interest: The authors declare that they have no conflicts of interest with regards to the contents of this article.

Ethical approval: This article does not contain any studies with human participants performed by any of the authors. All animal experiments were reviewed and approved by the University of Colorado Institutional Animal Care and Use Committee (IACUC) and performed under adherence to the ARVO Statement for the Use of Animals in Ophthalmic and Vision Research.

Carboxitin inhibited the glycation-mediated increase in stiffness in organ-cultured mouse lenses measured using compressive mechanical strain. Delivery of carboxitin into the lens increases GSH levels, traps dicarbonyl compounds and inhibits AGE formation. These properties of carboxitin could be exploited to develop a therapy against the formation of AGEs and the increase in stiffness that causes presbyopia in aging lenses.

Keywords

Carboxitin; lens; glycation; protein crosslinking; aging; presbyopia; mass spectrometry

Introduction

The human lens is a unique organ that facilitates the focusing of light onto the retina. Crystallins are the dominant proteins in the lens. The high concentration of crystallins helps the lens maintain a high refractive index. α -, β -, and γ -Crystallins in the lens, are among the longest-lived proteins in the human body [1] and account for 90% of the proteins in the lens [2]. α -Crystallin is made up of α A-crystallin (α AC) and α B-crystallin (α BC); these proteins exhibit chaperone activity that prevents the aggregation of proteins in aging lenses [3,4].

Because crystallins are exceptionally long-lived, their structural and functional integrity are considered vital for the lens to remain transparent during aging. However, with age, lens proteins become progressively crosslinked, water-insoluble and aggregated, resulting in increased light scattering [5]. Oxidative stress plays a major role in this process. As lenses age, the levels of GSH [6] and the activity of antioxidant enzymes decrease [7,8], resulting in increased oxidative modifications to proteins [9] that leads to the formation of intramolecular and intermolecular protein crosslinking by disulfide bonds [2]. Several other modifications, such as deamidation, truncation, racemization and glycation, also occur in crystallins during aging and are considered additional important contributing factors to lens aging [10–17].

Glycation is a reaction between reactive carbohydrates (containing aldehyde, keto and dicarbonyl groups) with the free amino groups of lysine and arginine residues in proteins. This reaction, through intermediates, forms diverse stable end products that are collectively known as advanced glycation end products or AGEs [18]. Some AGEs, such as carboxymethyllysine (CML), hydroimidazolone, and carboxyethyllysine (CEL), are formed as single amino acid modifications, and others, such as pentosidine, glucosepane, vesperlysine and methylglyoxal-lysine dimer (MOLD), are formed as amino acid crosslinked adducts. The crosslinking invariably involves two lysine residues (as in vesperlysine, MOLD) or lysine and arginine residues (as in pentosidine and glucosepane) [17]. The formation of such adducts alters the protein structure and function. AGEs progressively accumulate in aging human lenses and accumulate at higher levels in cataractous lenses [19–21]. In general, AGE levels are higher in highly crosslinked water-insoluble proteins than in less crosslinked water-soluble proteins of the lens [17,21,22], which implies that AGEs play a role in the protein crosslinking and aggregation that occurs

during lens aging and cataractogenesis. In addition, many AGEs are fluorescent and yellow/brown pigmented [23], the two characteristics that are similar to those of proteins in aged and cataractous lenses [24,25], further implicating AGEs in lens aging and cataract formation.

Methylglyoxal (MGO) and ascorbate (ASC) are considered major AGE precursors in the lens. MGO levels are regulated by the glyoxalase system, which is comprised of glyoxalase I and II [26]. Glyoxalase I converts the hemithioacetal formed from the nonenzymatic reaction of GSH and MGO to D-lactylglutathione, which is then converted to D-lactate by glyoxalase II [27]. In aging lenses, glyoxalase I protein levels and activity are decreased [26], which could promote the formation of AGEs from MGO [26,28]. ASC is present in relatively large quantities in human lenses (~2 mM) [23,17], possibly to protect the lens against oxidative damage. However, loss of GSH with aging leads the oxidation of ASC and a subsequent reduction in its levels [29–31]. The oxidation of ASC produces highly reactive glycating aldehydes and dicarbonyl compounds, such as erythrulose and 3-deoxythresosone (3-DT) [32]. These products are believed to be additional major precursors of AGEs in the lens. In support of a role for ASC in AGE formation, Dr. Monnier's laboratory elegantly demonstrated high levels of AGEs along with yellow pigmentation in the lenses of transgenic mice that specifically overexpressed a human Na⁺-dependent ascorbate transporter (hSVCT2) that had high levels of ASC and its oxidation products [33]. These observations imply that the loss of GSH and the formation of AGEs are major drivers of chemical modifications of proteins in aging lenses.

Chemical modifications in lens proteins are likely to be the major cause for the loss of accommodation due to an increase in stiffness during presbyopia in aging lenses. Presbyopia occurs between 40 and 50 years of age in many individuals and requires corrective lenses for reading [34]. It is estimated that ~1.8 billion people in the world have presbyopia [35]. Currently, there are no interventional or preventive medications against presbyopia. In 2016, Garner and Garner reported the development of a choline ester of lipoic acid to replenish GSH and decrease disulfide linkages in lens proteins in aged lenses. They showed that its topical application to the eye reduced stiffness in aged mouse lenses [36]. We reasoned that replenishing GSH alone might not be sufficient to inhibit age-associated stiffness in lenses, as that may not decrease dicarbonyl-mediated AGE formation, which is likely an additional important mechanism in lens stiffening.

With this in mind, we developed carboxitin, a molecule that contains GSH diester and mercaptoethylguanidine (MEG) linked by a disulfide bond (Fig. 1). The diester was introduced to increase the permeability across the plasma membrane, and MEG was introduced to simultaneously trap dicarbonyls. In this study, we investigated the ability of carboxitin to inhibit ASC-mediated AGE formation and protein crosslinking and the glycation-mediated increase in stiffness in organ-cultured mouse lenses.

Materials and methods

Materials

L-GSH (reduced) (cat# G6429), hydrogen chloride in dry ethanol (cat# 17934), cystamine dihydrochloride (cat# C121509), methylglyoxal (cat# 67028), erythrose (cat# 56845), ethylenediaminetetraacetic acid disodium salt dehydrate (EDTA) (cat# E5134), copper chloride (cat# 10125-13-0), L-ascorbic acid (cat# A7631), Chelex-100 (cat# C7901), O-phenylenediamine (OPD) (cat# 694975), and 1H-pyrazole-1-carboxamide HCl (cat# 402516) were purchased from Sigma-Aldrich (St. Louis, MO). Amberlite IRA 402 (OH⁻ form) (cat# A18185) was obtained from Alfa Aesar (Tewksbury, MA). CEL, CML, GOLD, GOLLA, MODIC and pentosidine were synthesized as previously described [37–42]. Antibody against α AC (cat# ADI-SPA-221-F) was obtained from Enzo Life Sciences (Farmingdale, NY). α BC antibody (cat# ABN185) was purchased from Millipore Sigma (Burlington, MA). Antibodies for β -crystallin (β -C) (cat# SC22745) and γ -crystallin (γ -C) (cat# SC22746) were obtained from Santa Cruz Biotechnology (Dallas, TX). HRP-conjugated anti-rabbit IgG (cat# 7074S) was purchased from Cell Signaling Technology (Danvers, MA). All other chemicals used were of analytical grade.

Synthesis of carboxitin

(a) Synthesis of GSH diethyl ester (GSH-OEt₂, 1)—GSH diethyl ester (**1**) was synthesized following a modified literature protocol [43]. Five hundred milligrams of reduced GSH (1.6 mmol) was dissolved in 10 ml of 0.5 M hydrogen chloride in dry ethanol. The solution was flushed with argon and stirred for 48 h at room temperature. Thereafter, the solvent was removed by vacuum centrifugation to yield crude product. Compound **1** was purified by preparative HPLC (Fig. 1) after dissolving approximately 60 mg of the crude product in 2 ml of water containing 0.1% trifluoroacetic acid (v/v) (solvent A). Individual fractions were analyzed by UPLC-MS². Fractions containing the product (m/z 364) were pooled and freeze-dried. Compound **1** was obtained as a colorless solid TFA salt. ¹H and ¹³C NMR spectra were obtained according to the literature [43].

(b) Synthesis of guanidinoethyl disulfide/mercaptoethylguanidine disulfide (2)—Mercaptoethylguanidine disulfide (**2**) was synthesized following a modified literature protocol [44]. Briefly, 500 mg of cystamine dihydrochloride (2.2 mmol) was dissolved in 25 ml of water. To this solution, 5 g of Amberlite IRA 402 (OH⁻ form) and 0.98 g of 1H-pyrazole-1-carboxamide HCl (6.6 mmol) were added. The mixture was stirred overnight at room temperature. The reaction mixture was extracted four times with 50 ml of ethyl acetate. The aqueous layer was acidified to pH 2 by the addition of 2 M HCl and freeze-dried. Compound **2** was obtained as a colorless solid hydrochloride salt. The ¹H and ¹³C NMR spectra were obtained according to the literature [44].

(c) Synthesis of carboxitin (GSH diethyl ester thioethylguanidine disulfide)—One hundred and ten milligrams of **1** (0.23 mmol) and 100 mg of **2** (0.32 mmol) were dissolved in 2 ml of 0.1 M phosphate buffer containing 1 mM EDTA. The solution was flushed with argon and incubated for 30 min at room temperature. Thereafter, the solution was adjusted to pH 2 with 1 M hydrochloric acid, to which 2 ml of solvent A (see below)

was added. Compound **3** was purified by preparative HPLC (Fig. 1). Individual fractions were analyzed by UPLC-MS² (see below). Fractions containing the product (*m/z* 481) were pooled and freeze-dried. Compound **3** was obtained as a colorless trifluoroacetate salt (40 mg, 0.06 mmol, 26%). The trifluoroacetic acid was removed by repeatedly dissolving **3** in 0.1% formic acid and subsequent freeze-drying. ¹H NMR (500 MHz, D₂O with 0.1% hydrochloric acid): 1.28 (t, J=6.7 Hz, 3H), 1.33 (t, J=6.7 Hz, 3H), 2.28 (m, 2H), 2.62 (m, 2H), 2.98 (m, 2H), 3.02 (m, 1H), 3.22 (m, 1H), 3.58 (t, J=6.6 Hz, 2H), 4.04 (m, 2H), 4.18 (t, J=6.7 Hz, 1H), 4.24 (q, J=6.8 Hz, 2H), 4.34 (q, J=6.6 Hz, 2H), 4.77 (interference with D₂O, confirmed by COSY, 1H). ¹³C NMR (125 MHz, D₂O with 0.1% hydrochloric acid): 13.8 (C14), 14.8 (C12), 26.4 (C3), 31.8 (C4), 37.1 (C15), 39.7 (C10), 40.8 (C16), 42.6 (C8), 53.1 (C2), 54.3 (C6), 63.7 (C13), 64.9 (C11), 158.0 (C17), 170.7 (C1), 172.4 (C9), 173.8 (C7), 175.3 (C5).

Preparative high-performance liquid chromatography purification of carboxitin intermediates and carboxitin

All preparative runs were carried out with a binary pump (Waters 1525, Milford, MA) operating at a flow rate of 15 ml/min. Samples were applied via a 2-ml injection loop (Rheodyne). Separations were carried out at room temperature on an RP C18 column (XBridge Prep C18, 250×19 mm, 5 μm; Waters) connected to a guard column. After the column, 0.3 ml/min was diverted through a valve to a UV-visible detector (Waters 2489), and the rest of the flow (14.7 ml/min) was collected in fractions. The following additional conditions were used for preparative purification of individual compounds. Water (solvent A) and 80% acetonitrile (solvent B (v/v)) were used as the eluents. To both solvents, 0.1% trifluoroacetic acid (v/v) was added. Analyses were performed using gradient elution: 10% B (0–5 min) to 20% B (20 min) to 30% B (25 min) to 70% B (35 min) to 100% B (40 to 55 min). The column was equilibrated with 10% B for 15 min prior to the next run. The detection wavelength was set to 230 nm. The fraction size was 14.7 ml.

Stability of carboxitin

To test the stability, carboxitin was incubated under various conditions. The following buffers were used: 0.1 M phosphate buffer pH 5, 0.1 M phosphate buffer pH 7, 0.1 M phosphate buffer pH 9 and 0.1% formic acid. A 10 μM solution of carboxitin in each buffer was stored at 4°C, 25°C or 37°C for up to 48 h. Sample aliquots were directly injected into UPLC-MS² for MRM analysis. For the identification of degradation products, sample aliquots were analyzed using full scan mode. All chromatographic analyses were carried out in a Waters Acquity UPLC system connected to a Sciex 4500 QTrap (Redwood City, CA). Mass spectrometric analyses were carried out in the multiple reaction monitoring (MRM) mode. Chromatographic separations were carried out in an ACQUITY BEH C18 peptide column (100 × 2.1 mm, 1.7 μm; Waters) connected to a guard column using a flow rate of 0.5 ml/min. Water (solvent A) and acetonitrile (solvent B) were used as the eluents. To both solvents, 0.1% heptafluorobutyric acid (v/v) was added. Analyses were performed at a column temperature of 40°C using gradient elution: 5% B (0–0.25 min) to 20% B (2 min) to 50% B (3 min) to 100% B (3.5–5 min). The column was equilibrated at 5% B for 1 min prior to the next analysis. Detection of the analytes was achieved by using full scan mode for the identification of the metabolites in the preparative HPLC fractions and multiple reaction

monitoring for quantitation in the stability experiments. The ion source was operated under the following conditions: temperature, 550°C; ion spray voltage, 4.5 kV; curtain gas, 45 ml/min; nebulizer gas, 60 ml/min; and heating gas, 60 ml/min. The mass range for full scan mode was set to 100–700 m/z , and the DP was set to 50 V. MRM parameters are presented in Table 1.

Testing for the entry of carboxitin into mouse and bovine lenses

All animal experiments were reviewed and approved by the University of Colorado Institutional Animal Care and Use Committee (IACUC) and performed under adherence to the ARVO Statement for the Use of Animals in Ophthalmic and Vision Research. Lenses from the eyes of C57BL/6J mice (5–6 months old) were isolated and incubated with carboxitin (2 mM) for 24 h at 37°C in serum-free and phenol red-free minimum essential medium (MEM). Homogenization buffer (PBS, 1.5 mM N-ethylmaleimide (NEM), pH 7) was added to each lens such that the buffer to tissue weight was 30 μ l of homogenization buffer/mg of wet tissue.

Bovine eyes were obtained from a local abattoir and transported to the laboratory within 6–10 h of sacrifice. Lenses were isolated and incubated with carboxitin (1.5 mM) for 24 h at 37°C in serum-free MEM. After 24 h, the medium was replaced with the fresh medium containing 1.5 mM carboxitin, and the lenses were incubated for another 24 h. A stainless steel pin was inserted through the center of the lens and immediately frozen in liquid nitrogen. By holding onto the pin, the lenses were shaved in a circular fashion from the outer cortex to the nucleus and collected as four fractions, arbitrarily named as the fractions from the outer cortex, middle cortex, inner cortex and nucleus. The shavings were weighed. To each fraction, homogenization buffer was added so that the buffer to tissue ratios was similar for all fractions (6 μ l of homogenization buffer/mg of wet tissue). The fractions were individually homogenized in homogenization buffer with a hand-held glass homogenizer, followed by sonication (30 sec each in 6 alternate cycles). The homogenates were kept at room temperature for 2 h for completion of NEM derivatization of the free thiols. The water-soluble fraction (WS) was obtained by centrifugation of the homogenate at 21,000 g for 20 min at 4°C. The WS was incubated with 10% trichloroacetic acid (TCA) for 0.5 h on ice and centrifuged at 21,000 g for 20 min at 4°C. The resulting supernatant was analyzed for carboxitin and its NEM-derivatized degradation products by UPLC-MS² as described above. The MRM parameters are shown in Table 1.

Effect of carboxitin on erythrose-mediated protein crosslinking in mouse lenses

Lenses from C57BL/6J mice (5–6 months old) were isolated, incubated with or without 2 mM carboxitin for 24 h at 37°C in serum-free MEM and then incubated with or without 2 mM erythrose for 72 h at 37°C in serum-free MEM in a CO₂ incubator. Lens stiffness was measured using a custom-made set up similar to that described by Fowler's laboratory [45,46]. Lenses were then homogenized in PBS and centrifuged at 21,000 g for 20 min at 4°C to obtain the WS. The WS was dialyzed against PBS for 16 h and analyzed by SDS-PAGE under reducing conditions using 4–20% gradient gels. To determine the crosslinking of the crystallins, the gels were electrophoretically transferred to a nitrocellulose membrane and incubated with one of the following antibodies: α AC antibody (dilution 1:5,000), α BC

antibody (dilution 1:5,000), β C antibody (dilution 1:2,000) or γ C antibody (dilution 1:2,000) for 16 h at 4°C. The membrane was then incubated with an HRP-conjugated anti-rabbit IgG (dilution 1:5,000) and developed using a SuperSignal West Pico or Femto kit (Pierce Chemicals, Rockford, IL).

Effect of carboxitin on erythrulose-mediated AGE synthesis in mouse lens proteins

The WS was acid- or enzyme-hydrolyzed as previously described [42]. All AGE standards were synthesized and characterized in Dr. Glomb's laboratory. The AGEs (GOLD, GOLA and GODIC) in the hydrolyzed lens WS proteins were determined as described previously [42]. The MRM parameters are shown in Table 2. Pentosidine (in the acid-hydrolyzed lens protein samples) was measured by UPLC as previously described [46].

Reaction of carboxitin with erythrulose-derived 3-deoxythreosone (3-DT)

Erythrulose at a 1 mM concentration was incubated with 1 mM carboxitin for 3 days at 37°C in 40 mM HEPES buffer pH 7. To the mixture, 5 mM OPD was added followed by incubation for 5 h at room temperature. The amount of 3-DT-quinoxaline formed was quantified by UPLC-MS². Additionally, 30 mM erythrulose was incubated alone for 2 days under the conditions described above, followed by dilution to 1 mM, to which 1 mM carboxitin was added and incubated for 24 h. OPD was then added to the assay mixture and incubated for 16 h, and the amount of 3-DT-quinoxaline formed was measured by UPLC-MS² as previously described [47].

Measurement of protein-free thiols in mouse lenses

To water-soluble mouse lens protein (3 mg/ml), TCA was added at a final concentration of 10% (W/V) to precipitate proteins. The free thiol content in the supernatant was estimated using 5,5'-dithiobis-(2-nitrobenzoic acid) (DTNB) in a microplate reader as previously described [48]. Briefly, 70 μ l of sample, 2.5 μ l of 4 mg/ml DTNB, and 177.5 μ l of 1 M Tris-EDTA buffer, pH 8.2 were incubated for 5 min at room temperature followed by measurement of the absorbance at 412 nm.

Measurement of glyoxalase-I activity in mouse lenses

The assay mixture consisting of 4.69 mM MGO and 250 mM GSH in buffer C (14.6 mM MgSO₄, 182 mM imidazole HCl, pH 7.2) was incubated for 30 min at room temperature. Mouse lens protein (5 μ g) was added to the mixture, and the change in absorbance was monitored for 30 min at 240 nm in a microplate reader. One unit of glyoxalase I activity was defined as 1 nmol of S-D-lactoyl glutathione formed/mg of protein/min.

Determination of the presence of glyoxal in erythrulose

Erythrulose (3 mM) solution was mixed with 30 mM OPD in 0.1% hydrochloric acid in 2 M sodium formate buffer (pH 3) containing 5 mM EDTA and incubated at 37°C for 16 h. To measure glyoxal-quinoxaline in mouse lenses, 30 μ l of 3 mg/ml protein solution was incubated with 0.35 mM OPD as described above. The incubation mixture was treated with TCA to a final concentration of 10% at 4°C for 2 h and centrifuged at 21,000 g for 20 min at 4°C. The supernatant was analyzed for glyoxal-quinoxaline using HPLC and a fluorescence

detector. The column was a Waters XBridge C18 5 μ M (4.6 \times 100 mm). A linear gradient program was used, with solvent A as 100% water with 0.1% formic acid and solvent B as 80% acetonitrile with 0.1% formic acid. The program was as follows: 0–5 min: 5% B; 5–10 min: 20% B; 10–25 min: 30% B; 25–30 min: 50% B; 30–35: 100% B, 35–40 min: 100% B; 40–45 min: 5% B; 45–50 min: 5% B; the flow rate was 1 ml/min. The column eluent was monitored with a fluorescence detector (excitation/emission wavelengths= 340/420 nm). The glyoxal-quinoxaline content in mouse lenses was quantified based on the standard curve for quinoxaline.

Statistical analysis

The data presented are the means \pm SD from experimental replicates as indicated in the figure legends. Student's *t*-test was used to analyze significant differences between groups using GraphPad Prism 7 software. A *p* value \leq 0.05 was considered statistically significant.

Results

Synthesis and stability of carboxitin

The synthesis strategy for carboxitin is shown in Fig. 1. Carboxitin was synthesized as a pure pale white product. We studied the stability of carboxitin under various conditions. Fig. 2 shows that carboxitin degraded in a time-dependent manner under most conditions, except for in 0.1% formic acid, where it was stable at all temperatures, at least for 48 h (Fig. 2A). At pH 5, carboxitin was stable at 4°C and 25°C but slightly degraded at 37°C (Fig. 2B). It degraded faster at elevated temperature and high pH. At pH 7 and 9, carboxitin degraded at all temperatures (Fig. 2C–D). Three degradation products of carboxitin were identified by mass spectrometry; the dominant degradation pathway was the loss of either one or two ethanol moieties from the terminal carboxyl groups (Fig. 2E). Therefore, there were two degradation products with the loss of one molecule ethanol (glutamic acid side or glycine side) and one with the loss of two molecules of ethanol (glutamic acid side and glycine side) (Fig. 2E). Both degradation products were monitored in the stability tests (Fig. 2F–G). During incubation under the conditions described above, reduction of the disulfide bond was not observed.

Carboxitin is permeable to bovine and mouse lenses

UPLC-MS² analysis of the four fractions of bovine lenses showed that upon incubation with carboxitin for 48 h, the GSH and GSH monoester-NEM levels increased in the nuclei of the lenses; the carboxitin-treated lenses had GSH levels in the nuclear fraction that were 2.5-fold higher than those of the untreated lenses (Fig. 3A). In all other fractions, the GSH (as an NEM derivative) levels were similar. The GSH monoester-NEM (1 and 2) levels were 4.6- and 16.7-fold higher in the nucleus of carboxitin-treated lenses than in untreated lenses (Fig. 3A). GSH monoester-NEM (1) was found to be 2.7- and 1.5-fold and GSH monoester-NEM (2) was 23- and 8.5-fold higher in the outer and middle cortical regions of carboxitin-treated lenses, respectively, compared with untreated lenses. However, both of these esters were found to be similar in the inner cortex for carboxitin-treated or untreated lenses. The GSH diester was found to be similar in all fractions except for the outer cortex, where it was found to be 400-fold higher in carboxitin-treated lenses than in untreated lenses (Fig. 3A).

While the untreated lenses had no MEG (as an NEM derivative) in any of the four fractions, in carboxitin-treated lenses, we found MEG in the outer cortex, middle cortex, inner cortex and nuclear fractions. The levels of carboxitin in carboxitin-treated bovine lenses were below the limits of detection. Altogether, the results showed that upon entering the lenses, carboxitin is reduced and de-esterified into GSH, GSH monoesters, GSH diesters and MEG.

UPLC-MS² analysis of mouse lenses incubated with carboxitin for 24 h showed carboxitin, MEG-NEM, GSH monoester-NEM and GSH diester-NEM (Fig. 3B). These results suggest that carboxitin can penetrate mouse lenses. Upon entering mouse lenses, carboxitin is reduced and forms GSH mono- and diesters and MEG. Longer incubation of mouse lenses with carboxitin (1 day) and subsequent incubation with or without erythrose (3 days) showed 2.85- and 1.7-fold higher levels of free thiols, respectively, than lenses that were not incubated with carboxitin (Fig. 3C).

Carboxitin suppresses AGE formation in mouse lenses

Incubation of mouse lenses with erythrose for 72 h caused significant increases in the levels of protein crosslinking AGEs, GODIC (0.43 ± 0.1 pmol/ μ mol leucine equivalents, $p < 0.05$) and pentosidine (0.11 ± 0.02 pmol/ μ mol, $p < 0.0001$) compared to untreated lenses (Fig. 4A). The GOLD (0.11 ± 0.03 pmol/ μ mol) and GOLA levels (0.4 ± 0.05 pmol/ μ mol) also showed an increasing trend but were not statistically significant when compared to the control. Lenses that were preincubated with carboxitin for 24 h and then incubated with erythrose for 72 h had 0.06 ± 0.03 and 0.08 ± 0.02 pmol/ μ mol leucine equivalents of GOLD and pentosidine, respectively. These values were 43% ($p < 0.05$) and 29% ($p < 0.05$) lower than lenses treated with erythrose alone. However, no significant differences in the levels of GOLA (0.6 ± 0.24 pmol/ μ mol) and GODIC (0.6 ± 0.26 pmol/ μ mol) were found in lenses treated with carboxitin + erythrose compared to lenses treated with erythrose alone (GOLA: 0.4 ± 0.05 and GODIC: 0.43 ± 0.1 pmol/ μ mol). The CML levels in lenses treated with erythrose were significantly ($p < 0.0001$) higher (138.683 ± 10.1 pmol/ μ mol) than the control (59.5 ± 7.4 pmol/ μ mol). Preincubation of lenses with carboxitin followed by incubation with erythrose resulted in significantly ($p < 0.05$) lower levels of CML (109.7 ± 21 pmol/ μ mol). Altogether, our findings suggest that carboxitin suppresses the accumulation of AGEs in mouse lenses.

The increase in crosslinked AGE formation in erythrose-incubated lenses was not due to a loss of glyoxalase I activity, as the enzymatic activity was not significantly different between control and erythrose-incubated lenses (Fig. 4B). The enzymatic activity was unaltered with the addition of carboxitin in the presence or absence of erythrose. Furthermore, to determine whether the increase in GOLD and GODIC in lenses incubated with erythrose was due to an increase in glyoxal in the lens, we measured glyoxal as a quinoxaline derivative. We found that glyoxal-quinoxaline was significantly ($p < 0.05$) increased in erythrose-treated lenses and significantly reduced ($p < 0.05$) upon treatment with carboxitin. This could be due to the formation of glyoxal from erythrose in mouse lenses. Another possibility was that glyoxal could be present in erythrose (from Sigma-Aldrich) as a contaminant. We investigated this possibility by treating erythrose with OPD and measuring glyoxal-quinoxaline by HPLC. On a molar basis, we found ~5% erythrose to be

glyoxal (Supplementary Fig. 1). Upon preincubating erythrulose with aminoguanidine hydrochloride at a ratio of 1:1 (M/M), the peak for glyoxal-quinoxaline was quenched (Supplementary Fig. 1), which confirmed the presence of glyoxal in the commercial preparation of erythrulose.

Carboxitin inhibits protein crosslinking in mouse lenses

Treatment of organ-cultured mouse lenses with 2 mM erythrulose for 3 days resulted in 25% higher levels of crosslinked proteins than untreated lenses (Fig. 5). Treatment with carboxitin for 24 h followed by treatment with erythrulose for 72 h reduced this crosslinking by 45%. To determine the crosslinking of individual crystallins, western blotting for α AC, α BC, β C and γ C was performed. Erythrulose caused crosslinking in all these crystallins, but carboxitin reduced the crosslinking by 11.6, 47, 34 and 34%, respectively. These observations suggest that carboxitin, upon entering lenses, prevents the glycation-mediated crosslinking of proteins.

Carboxitin traps 3-DT

To understand how carboxitin prevents protein crosslinking and suppresses AGE formation, we tested its ability to trap 3-DT, which is the most abundant dicarbonyl compound formed from ASC degradation. The ASC oxidation product erythrulose is a major precursor of 3-DT [32]. Therefore, we used erythrulose as a source of 3-DT in the incubation experiment. Incubation of erythrulose alone for 3 days produced 3-DT (measured as a quinoxaline derivative, 3-DT-Q) (Fig. 6A). However, when erythrulose was incubated with carboxitin, the 3-DT levels were 47.5% lower ($p < 0.0001$). After 2 days of preincubation with erythrulose followed by incubation for an additional day in the presence of carboxitin, 3-DT levels were again significantly ($p < 0.01$) reduced; this time, the reduction was 25% (Fig. 6B). These results imply that carboxitin inhibits erythrulose-mediated AGE formation by trapping 3-DT.

Carboxitin inhibits glycation-mediated increase in mouse lens stiffness

The compressive stiffness of mouse lenses incubated with or without carboxitin was measured. In lenses incubated with carboxitin, there were significant increase in the axial and equatorial strain by 21% ($p < 0.05$) and 43% ($p < 0.01$), respectively, compared to untreated control lenses (Fig. 7). Upon incubation with erythrulose, the axial and equatorial strains of the lenses were significantly decreased by 23% ($p < 0.05$) and 28% ($p < 0.05$), respectively, compared to control lenses. However, in lenses that were pretreated with carboxitin and then treated with erythrulose, there was a 32% ($p < 0.05$) and 48% ($p < 0.05$) increase in the axial and equatorial strains, respectively, when compared to lenses treated with erythrulose alone. Together, these results imply that carboxitin is able to inhibit both pre-existing and AGE-mediated stiffness in mouse lenses.

Discussion

The objectives of this study were 1) to determine the ability of carboxitin to permeate the lenses and inhibit AGE formation and 2) to investigate the ability of carboxitin to reduce lens stiffness.

Carboxitin was developed to target three modulators of AGE synthesis at the same time: 1) ASC oxidation, 2) glyoxalase I activity and 3) dicarbonyl stress. We used GSH diethyl ester to enhance the permeability of carboxitin across the plasma membrane of cells. Guanidine is generally impermeable to the plasma membrane. With the attachment of MEG to the GSH diester, we expected its entrance into cells. We anticipated that reduction of the disulfide bond in carboxitin would release GSH diester and MEG once inside the lenses. The GSH diester would then be de-esterified by an esterase to release GSH. Our experiments clearly showed that carboxitin enters mouse lenses and is reduced to form GSH mono- and diesters and mercaptoethylguanidine. In bovine lenses, we observed higher levels of GSH, glutathione monoesters and MEG in the nucleus, clearly showing the permeation of carboxitin into the nucleus of the lens.

3-DT is the most abundant dicarbonyl compound in human lenses and is formed from erythrose, an intermediate of ASC oxidation and degradation [47,32]. We found that carboxitin was able to significantly reduce the 3-DT levels in mouse lenses that were incubated with erythrose. In addition, carboxitin was also able to inhibit erythrose-mediated protein crosslinking and AGE formation in mouse lenses. Taken together, these observations strongly suggest that carboxitin could be used to prevent dicarbonyl-mediated AGE formation in the lens. In addition to 3-DT, GO is a significant AGE precursor in tissues [17,32]. The GSH-dependent glyoxalase system metabolizes GO to glycolate [49,27]. The inhibition of CML and GOLD suggests that the delivery of carboxitin trapped glyoxal and possibly increased its metabolism by improving glyoxalase I activity in the lens. However, a surprising finding was the ineffectiveness of carboxitin to suppress the levels of GOLA and GODIC in lenses treated with erythrose. These two AGEs are likely derived from glyoxal, which is similar to CML and GOLD. It is possible that the synthetic rate for GOLA and GODIC exceeded the rate of inhibition by carboxitin, resulting in the inability of carboxitin to suppress their formation. However, further experiments are required to understand this dichotomous effect of carboxitin.

Despite presbyopia being a major visual impairment in most middle-aged adults, there are currently no FDA-approved medications to prevent, intervene or reverse this condition. While surgical removal of the presbyopic lens and replacement with an intraocular lens is an option, this procedure is cost-prohibitive in most parts of the world.

This has prompted investigations into preventing/reversing presbyopia with topical medications. A recent study showed that topical application of a combination of nonsteroidal anti-inflammatory drugs improves near vision in human subjects, possibly through the correction of presbyopia [50]. The US patent registry lists several other small molecules to treat presbyopia, but the one that has advanced to human clinical trials is the choline ester of lipoic acid that Garner and Garner [36] developed through Novartis. Carboxitin is potentially a significant additional small molecule inhibitor against presbyopia. We found that carboxitin, upon entering the lens, was degraded to GSH mono- and diesters and MEG. An interesting observation in our study is the ability of carboxitin to reduce stiffness in mouse lenses that were not treated with erythrose. It is possible that the GSH derived from carboxitin promoted the reduction of the disulfide crosslinks in lens proteins and decreased the stiffness. In addition, preincubation of the lenses with carboxitin and subsequent

treatment with erythrose significantly reduced lens stiffness. The fact that carboxitin blocked crosslinked AGE formation during this process implicates AGEs in the promotion of lens stiffness. GSH derived from carboxitin could prevent ASC oxidation through the reduction of dehydroascorbate and prevent the formation of AGE precursors. Carboxitin could also reduce the levels of AGE precursors, such as MGO, by trapping them with MEG and by increasing their metabolism through glyoxalase by enhancing GSH levels. These combined effects (in addition to the reduction of disulfide bonds) could be the reasons for the reduction of stiffness in erythrose-incubated lenses.

In summary, carboxitin can inhibit protein crosslinking and AGE accumulation in lens proteins. More importantly, at least *in vitro*, carboxitin could be delivered into lenses, reaching the inner nucleus and reducing lens stiffness. Our study suggests that carboxitin exhibits these properties through multiple mechanisms, such as trapping dicarbonyl compounds and possibly increasing glyoxalase activity. We believe that carboxitin could be developed as a small molecule therapeutic agent to prevent presbyopia and possibly cataracts.

Supplementary Material

Refer to Web version on PubMed Central for supplementary material.

Acknowledgment

The authors thank Saving Sight, Kansas City, MO, for providing the human lenses.

Funding information

This work was supported by the National Institutes of Health Grants EY028836 and EY023286 (RHN) and an RPB challenge grant to the Department of Ophthalmology, University of Colorado.

References

1. McAvoy JW, Chamberlain CG, de Iongh RU, Hales AM, Lovicu FJ: Lens development. *Eye (Lond)* 13 (Pt 3b), 425–437 (1999). doi:10.1038/eye.1999.117 [PubMed: 10627820]
2. Sharma KK, Santhoshkumar P: Lens aging: effects of crystallins. *Biochim Biophys Acta* 1790(10), 1095–1108 (2009). doi:10.1016/j.bbagen.2009.05.008 [PubMed: 19463898]
3. Andley UP: Crystallins in the eye: Function and pathology. *Prog Retin Eye Res* 26(1), 78–98 (2007). doi:10.1016/j.preteyeres.2006.10.003 [PubMed: 17166758]
4. Horwitz J: Alpha-crystallin can function as a molecular chaperone. *Proc Natl Acad Sci U S A* 89(21), 10449–10453 (1992). doi:10.1073/pnas.89.21.10449 [PubMed: 1438232]
5. Petrash JM: Aging and age-related diseases of the ocular lens and vitreous body. *Invest Ophthalmol Vis Sci* 54(14), ORSF54–59 (2013). doi:10.1167/iovs.13-12940 [PubMed: 24335070]
6. Harding JJ: Free and protein-bound glutathione in normal and cataractous human lenses. *Biochem J* 117(5), 957–960 (1970). doi:10.1042/bj1170957 [PubMed: 5451916]
7. Bonet Serra B, Barrio Merino A, Quintanar Rioja A, Alaves Buforn M, Nevado Santos M: [Steatosis and cirrhosis secondary to insulin resistance in children. Possible physiopathological mechanisms]. *An Esp Pediatr* 56(4), 353–356 (2002). [PubMed: 11927081]
8. Chang D, Zhang X, Rong S, Sha Q, Liu P, Han T, Pan H: Serum antioxidative enzymes levels and oxidative stress products in age-related cataract patients. *Oxid Med Cell Longev* 2013, 587826 (2013). doi:10.1155/2013/587826 [PubMed: 23781296]

9. Taylor A, Davies KJ: Protein oxidation and loss of protease activity may lead to cataract formation in the aged lens. *Free Radic Biol Med* 3(6), 371–377 (1987). doi:10.1016/0891-5849(87)90015-3 [PubMed: 3322949]
10. Gakamsky A, Duncan RR, Howarth NM, Dhillon B, Buttenschon KK, Daly DJ, Gakamsky D: Tryptophan and Non-Tryptophan Fluorescence of the Eye Lens Proteins Provides Diagnostics of Cataract at the Molecular Level. *Sci Rep* 7, 40375 (2017). doi:10.1038/srep40375 [PubMed: 28071717]
11. Hains PG, Truscott RJ: Age-dependent deamidation of lifelong proteins in the human lens. *Invest Ophthalmol Vis Sci* 51(6), 3107–3114 (2010). doi:10.1167/iovs.09-4308 [PubMed: 20053973]
12. Hooi MY, Truscott RJ: Racemisation and human cataract. D-Ser, D-Asp/Asn and D-Thr are higher in the lifelong proteins of cataract lenses than in age-matched normal lenses. *Age (Dordr)* 33(2), 131–141 (2011). doi:10.1007/s11357-010-9171-7 [PubMed: 20686926]
13. Kumar MS, Koteiche HA, Claxton DP, McHaourab HS: Disulfide cross-links in the interaction of a cataract-linked alphaA-crystallin mutant with betaB1-crystallin. *FEBS Lett* 583(1), 175–179 (2009). doi:10.1016/j.febslet.2008.11.047 [PubMed: 19071118]
14. Lund AL, Smith JB, Smith DL: Modifications of the water-insoluble human lens alpha-crystallins. *Exp Eye Res* 63(6), 661–672 (1996). doi:10.1006/exer.1996.0160 [PubMed: 9068373]
15. Kodama T, Takemoto L: Characterization of disulfide-linked crystallins associated with human cataractous lens membranes. *Invest Ophthalmol Vis Sci* 29(1), 145–149 (1988). [PubMed: 3335427]
16. Garlick RL, Mazer JS, Chylack LT Jr., Tung WH, Bunn HF: Nonenzymatic glycation of human lens crystallin. Effect of aging and diabetes mellitus. *J Clin Invest* 74(5), 1742–1749 (1984). doi:10.1172/JCI111592 [PubMed: 6438156]
17. Nagaraj RH, Linetsky M, Stitt AW: The pathogenic role of Maillard reaction in the aging eye. *Amino Acids* 42(4), 1205–1220 (2012). doi:10.1007/s00726-010-0778-x [PubMed: 20963455]
18. Monnier VM, Nagaraj RH, Portero-Otin M, Glomb M, Elgawish AH, Sell DR, Friedlander MA: Structure of advanced Maillard reaction products and their pathological role. *Nephrol Dial Transplant* 11 Suppl 5, 20–26 (1996). doi:10.1093/ndt/11.supp5.20
19. Biemel KM, Friedl DA, Lederer MO: Identification and quantification of major maillard cross-links in human serum albumin and lens protein. Evidence for glucosepane as the dominant compound. *J Biol Chem* 277(28), 24907–24915 (2002). doi:10.1074/jbc.M202681200 [PubMed: 11978796]
20. Lyons TJ, Silvestri G, Dunn JA, Dyer DG, Baynes JW: Role of glycation in modification of lens crystallins in diabetic and nondiabetic senile cataracts. *Diabetes* 40(8), 1010–1015 (1991). doi:10.2337/diab.40.8.1010 [PubMed: 1907246]
21. Nagaraj RH, Sell DR, Prabhakaram M, Ortwerth BJ, Monnier VM: High correlation between pentosidine protein crosslinks and pigmentation implicates ascorbate oxidation in human lens senescence and cataractogenesis. *Proc Natl Acad Sci U S A* 88(22), 10257–10261 (1991). doi:10.1073/pnas.88.22.10257 [PubMed: 1946446]
22. Tessier F, Obrenovich M, Monnier VM: Structure and mechanism of formation of human lens fluorophore LM-1. Relationship to vesperlysine A and the advanced Maillard reaction in aging, diabetes, and cataractogenesis. *J Biol Chem* 274(30), 20796–20804 (1999). doi:10.1074/jbc.274.30.20796 [PubMed: 10409619]
23. Cheng R, Lin B, Lee KW, Ortwerth BJ: Similarity of the yellow chromophores isolated from human cataracts with those from ascorbic acid-modified calf lens proteins: evidence for ascorbic acid glycation during cataract formation. *Biochim Biophys Acta* 1537(1), 14–26 (2001). doi:10.1016/s0925-4439(01)00051-5 [PubMed: 11476959]
24. Bron AJ, Vrensen GF, Koretz J, Maraini G, Harding JJ: The ageing lens. *Ophthalmologica* 214(1), 86–104 (2000). doi:10.1159/000027475 [PubMed: 10657747]
25. de Jong WW, Mulders JW, Voorter CE, Berbers GA, Hoekman WA, Bloemendal H: Post-translational modifications of eye lens crystallins: crosslinking, phosphorylation and deamidation. *Adv Exp Med Biol* 231, 95–108 (1988). doi:10.1007/978-1-4684-9042-8_8 [PubMed: 2901197]
26. Haik GM Jr., Lo TW, Thornalley PJ: Methylglyoxal concentration and glyoxalase activities in the human lens. *Exp Eye Res* 59(4), 497–500 (1994). doi:10.1006/exer.1994.1135 [PubMed: 7859825]

27. Thornalley PJ: The glyoxalase system in health and disease. *Mol Aspects Med* 14(4), 287–371 (1993). doi:10.1016/0098-2997(93)90002-u [PubMed: 8277832]
28. Shamsi FA, Lin K, Sady C, Nagaraj RH: Methylglyoxal-derived modifications in lens aging and cataract formation. *Invest Ophthalmol Vis Sci* 39(12), 2355–2364 (1998). [PubMed: 9804144]
29. Kusic B, Miric D, Zoric L, Ilic A, Dragojevic I: Antioxidant capacity of lenses with age-related cataract. *Oxid Med Cell Longev* 2012, 467130 (2012). doi:10.1155/2012/467130 [PubMed: 22363833]
30. Reddy VN: Glutathione and its function in the lens--an overview. *Exp Eye Res* 50(6), 771–778 (1990). doi:10.1016/0014-4835(90)90127-g [PubMed: 2197112]
31. Sasaki H, Giblin FJ, Winkler BS, Chakrapani B, Leverenz V, Shu CC: A protective role for glutathione-dependent reduction of dehydroascorbic acid in lens epithelium. *Invest Ophthalmol Vis Sci* 36(9), 1804–1817 (1995). [PubMed: 7635655]
32. Nemet I, Monnier VM: Vitamin C degradation products and pathways in the human lens. *J Biol Chem* 286(43), 37128–37136 (2011). doi:10.1074/jbc.M111.245100 [PubMed: 21885436]
33. Fan X, Reneker LW, Obrenovich ME, Strauch C, Cheng R, Jarvis SM, Ortwerth BJ, Monnier VM: Vitamin C mediates chemical aging of lens crystallins by the Maillard reaction in a humanized mouse model. *Proc Natl Acad Sci U S A* 103(45), 16912–16917 (2006). doi:10.1073/pnas.0605101103 [PubMed: 17075057]
34. du Toit R: How to prescribe spectacles for presbyopia. *Community Eye Health* 19(57), 12–13 (2006). [PubMed: 17491738]
35. Fricke TR, Tahhan N, Resnikoff S, Papas E, Burnett A, Ho SM, Naduvilath T, Naidoo KS: Global Prevalence of Presbyopia and Vision Impairment from Uncorrected Presbyopia: Systematic Review, Meta-analysis, and Modelling. *Ophthalmology* 125(10), 1492–1499 (2018). doi:10.1016/j.ophtha.2018.04.013 [PubMed: 29753495]
36. Garner WH, Garner MH: Protein Disulfide Levels and Lens Elasticity Modulation: Applications for Presbyopia. *Invest Ophthalmol Vis Sci* 57(6), 2851–2863 (2016). doi:10.1167/iovs.15-18413 [PubMed: 27233034]
37. Fujioka M, Tanaka M: Enzymic and chemical synthesis of epsilon-N-(L-propionyl-2)-L-lysine. *Eur J Biochem* 90(2), 297–300 (1978). doi:10.1111/j.1432-1033.1978.tb12603.x [PubMed: 361398]
38. Glomb MA, Monnier VM: Mechanism of protein modification by glyoxal and glycolaldehyde, reactive intermediates of the Maillard reaction. *J Biol Chem* 270(17), 10017–10026 (1995). doi:10.1074/jbc.270.17.10017 [PubMed: 7730303]
39. Glomb MA, Pfahler C: Amides are novel protein modifications formed by physiological sugars. *J Biol Chem* 276(45), 41638–41647 (2001). doi:10.1074/jbc.M103557200 [PubMed: 11493602]
40. Lederer MO, Klaiber RG: Cross-linking of proteins by Maillard processes: characterization and detection of lysine-arginine cross-links derived from glyoxal and methylglyoxal. *Bioorg Med Chem* 7(11), 2499–2507 (1999). doi:10.1016/s0968-0896(99)00212-6 [PubMed: 10632059]
41. Sell DR, Monnier VM: Structure elucidation of a senescence cross-link from human extracellular matrix. Implication of pentoses in the aging process. *J Biol Chem* 264(36), 21597–21602 (1989). [PubMed: 2513322]
42. Smuda M, Henning C, Raghavan CT, Johar K, Vasavada AR, Nagaraj RH, Glomb MA: Comprehensive analysis of maillard protein modifications in human lenses: effect of age and cataract. *Biochemistry* 54(15), 2500–2507 (2015). doi:10.1021/bi5013194 [PubMed: 25849437]
43. Thornalley PK: Esterification of reduced glutathione. *Biochem J* 275 (Pt 2), 535–539 (1991). doi:10.1042/bj2750535 [PubMed: 2025232]
44. Szabo C, Bryk R, Zingarelli B, Southan GJ, Gahman TC, Bhat V, Salzman AL, Wolff DJ: Pharmacological characterization of guanidinoethylidithiolane (GED), a novel inhibitor of nitric oxide synthase with selectivity towards the inducible isoform. *Br J Pharmacol* 118(7), 1659–1668 (1996). doi:10.1111/j.1476-5381.1996.tb15589.x [PubMed: 8842429]
45. Cheng C, Gokhin DS, Nowak RB, Fowler VM: Sequential Application of Glass Coverslips to Assess the Compressive Stiffness of the Mouse Lens: Strain and Morphometric Analyses. *J Vis Exp*(111) (2016). doi:10.3791/53986
46. Nandi SK, Nahomi RB, Rankenberg J, Glomb MA, Nagaraj RH: Glycation-mediated inter-protein cross-linking is promoted by chaperone-client complexes of alpha-crystallin: Implications for lens

- aging and presbyopia. *J Biol Chem* 295(17), 5701–5716 (2020). doi:10.1074/jbc.RA120.012604 [PubMed: 32184356]
47. Rakete S, Nagaraj RH: Identification of Kynoxazine, a Novel Fluorescent Product of the Reaction between 3-Hydroxykynurenine and Erythrulose in the Human Lens, and Its Role in Protein Modification. *J Biol Chem* 291(18), 9596–9609 (2016). doi:10.1074/jbc.M116.716621 [PubMed: 26941078]
48. Gangadhariah MH, Mailankot M, Reneker L, Nagaraj RH: Inhibition of methylglyoxal-mediated protein modification in glyoxalase I overexpressing mouse lenses. *J Ophthalmol* 2010, 274317 (2010). doi:10.1155/2010/274317 [PubMed: 20671953]
49. Lange JN, Wood KD, Knight J, Assimos DG, Holmes RP: Glyoxal formation and its role in endogenous oxalate synthesis. *Adv Urol* 2012, 819202 (2012). doi:10.1155/2012/819202 [PubMed: 22567004]
50. Renna A, Vejarano LF, De la Cruz E, Alio JL: Pharmacological Treatment of Presbyopia by Novel Binocularly Instilled Eye Drops: A Pilot Study. *Ophthalmol Ther* 5(1), 63–73 (2016). doi:10.1007/s40123-016-0050-x [PubMed: 27168149]

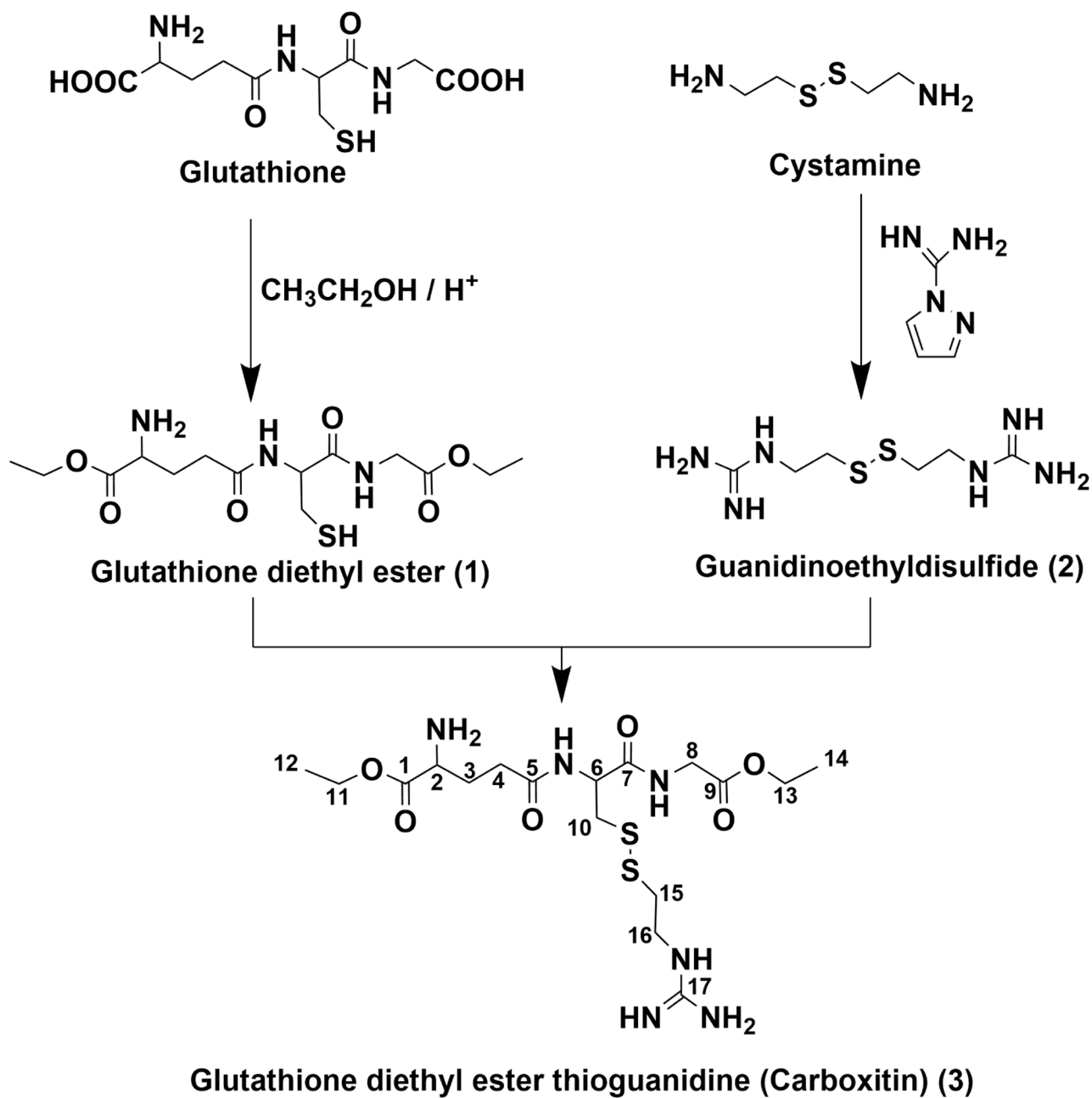


Fig. 1. Synthesis strategy of carboxitin.

The yield of carboxitin was 11 mg, starting from 500 mg of GSH.

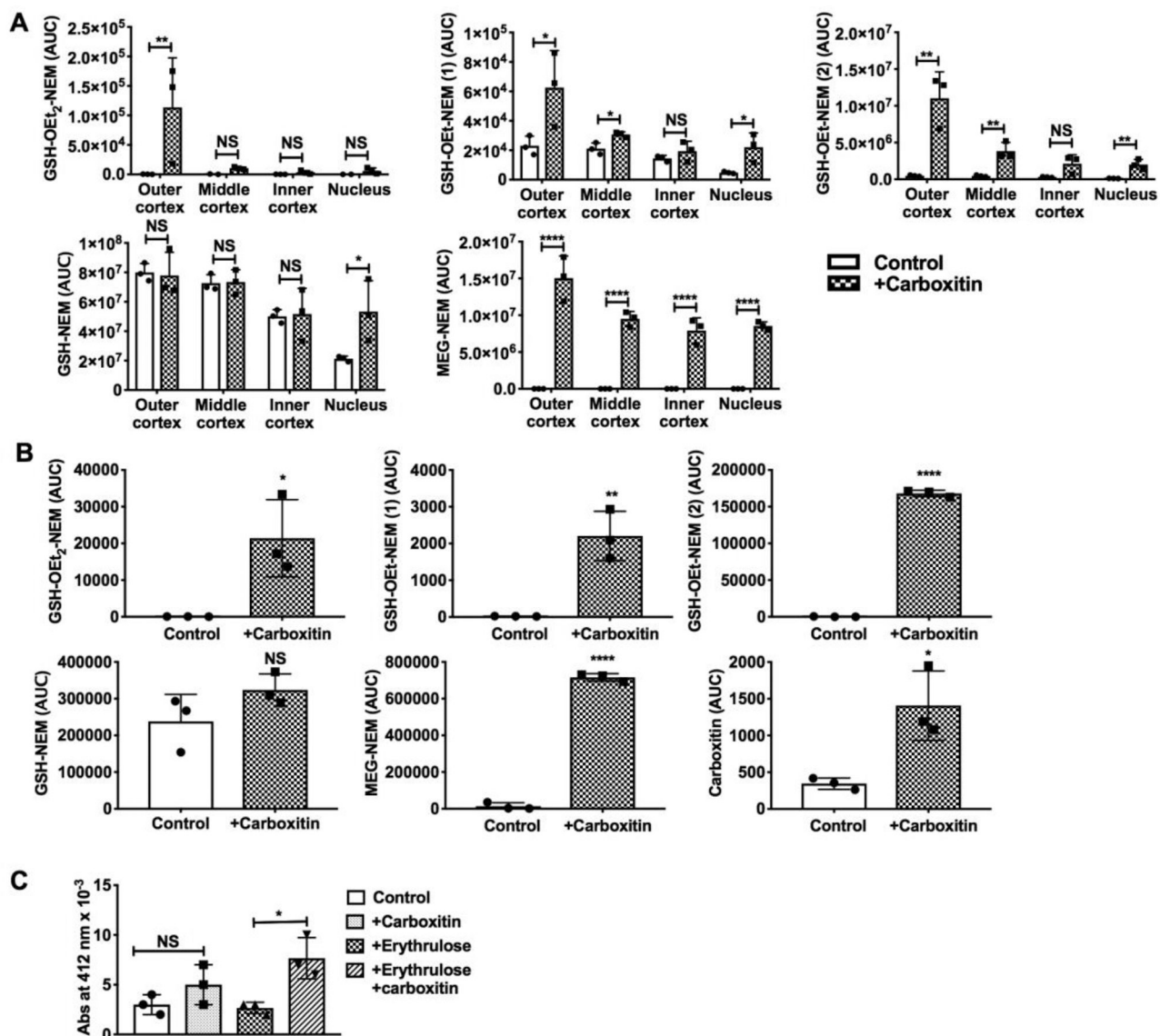


Fig. 3. Carboxitin permeates bovine and mouse lenses.

(A) UPLC-MS² analysis of bovine lens fractions for GSH-NEM and MEG-NEM. The lenses were incubated with 1.5 mM carboxitin for 48 h at 37°C prior to analysis. (B) WS mouse lens analysis by UPLC-MS² for carboxitin, MEG-NEM, GSH-OEt₂-NEM, GSH-OEt-NEM (1), and GSH-OEt-NEM (2). The lenses were incubated with 2 mM carboxitin for 24 h at 37°C prior to analysis. (C) Thiol estimation using the DTNB assay in mouse lenses treated with or without 2 mM carboxitin for 24 h and then treated with or without erythrulose for another 3 days at 37°C in a CO₂ incubator. Bar graphs represent the means ± SD of triplicate measurements. NS, not significant; *p<0.05; **p<0.01; ****p<0.0001.

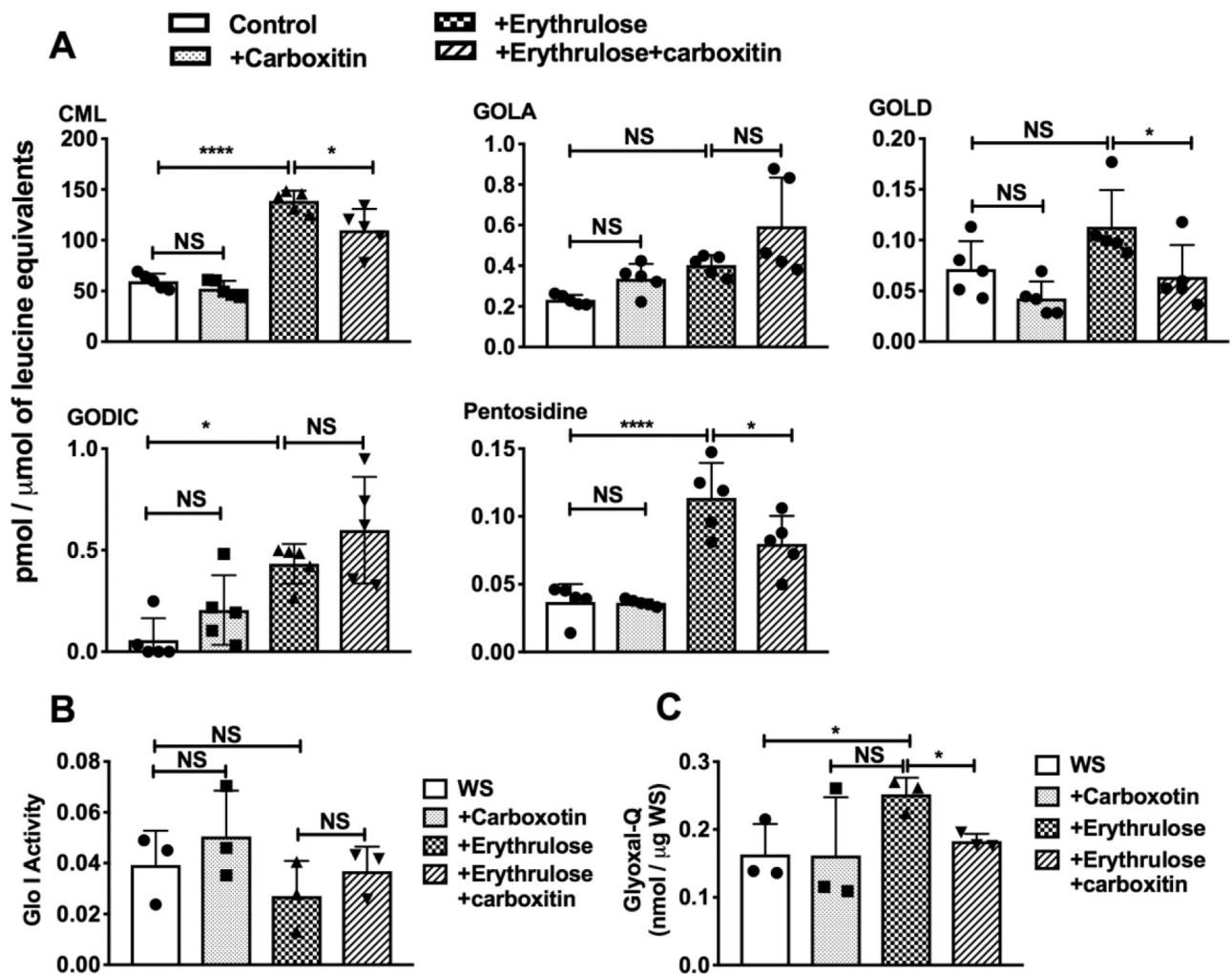


Fig. 4. Carboxitin inhibits AGE formation in mouse lenses.

(A) WS of mouse lenses that were subjected to erythulose treatment in the presence or absence of carboxitin were analyzed by UPLC-MS² for the crosslinking of AGEs. (B) Glyoxalase-I activity in the WS from lenses treated with erythulose. (C) Glyoxal in erythulose-incubated lenses measured as a quinoxaline derivative (glyoxal-Q). Bar graphs represent the means \pm SD of triplicate measurements. NS, not significant; * p <0.05; **** p <0.0001.

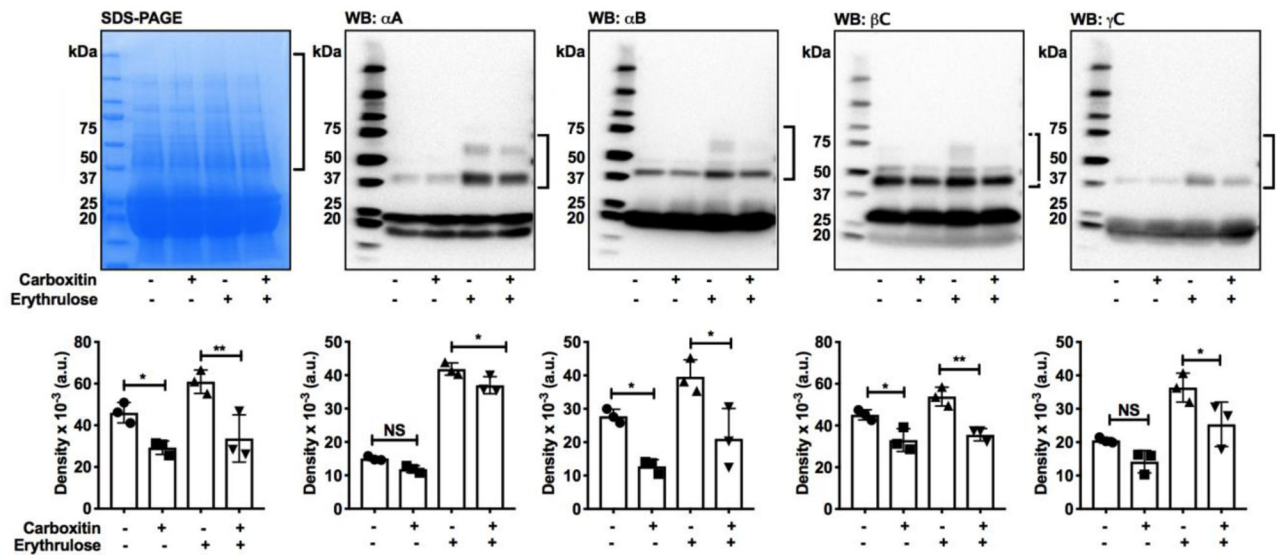


Fig. 5. Carboxitin inhibits erythrulose-mediated crosslinking of mouse lens proteins.

The WS from mouse lenses that were glycosylated using erythrulose in the presence or absence of carboxitin were run on 4–20% SDS-PAGE. Western blots against α AC, α BC, β C and γ C revealed the formation of intermolecular crosslinking. Densitometry of the regions marked by brackets in the SDS-PAGE and western blots are also shown. Bar graphs represent the means \pm SD of triplicate measurements. NS, not significant; *p<0.05; **p<0.01.

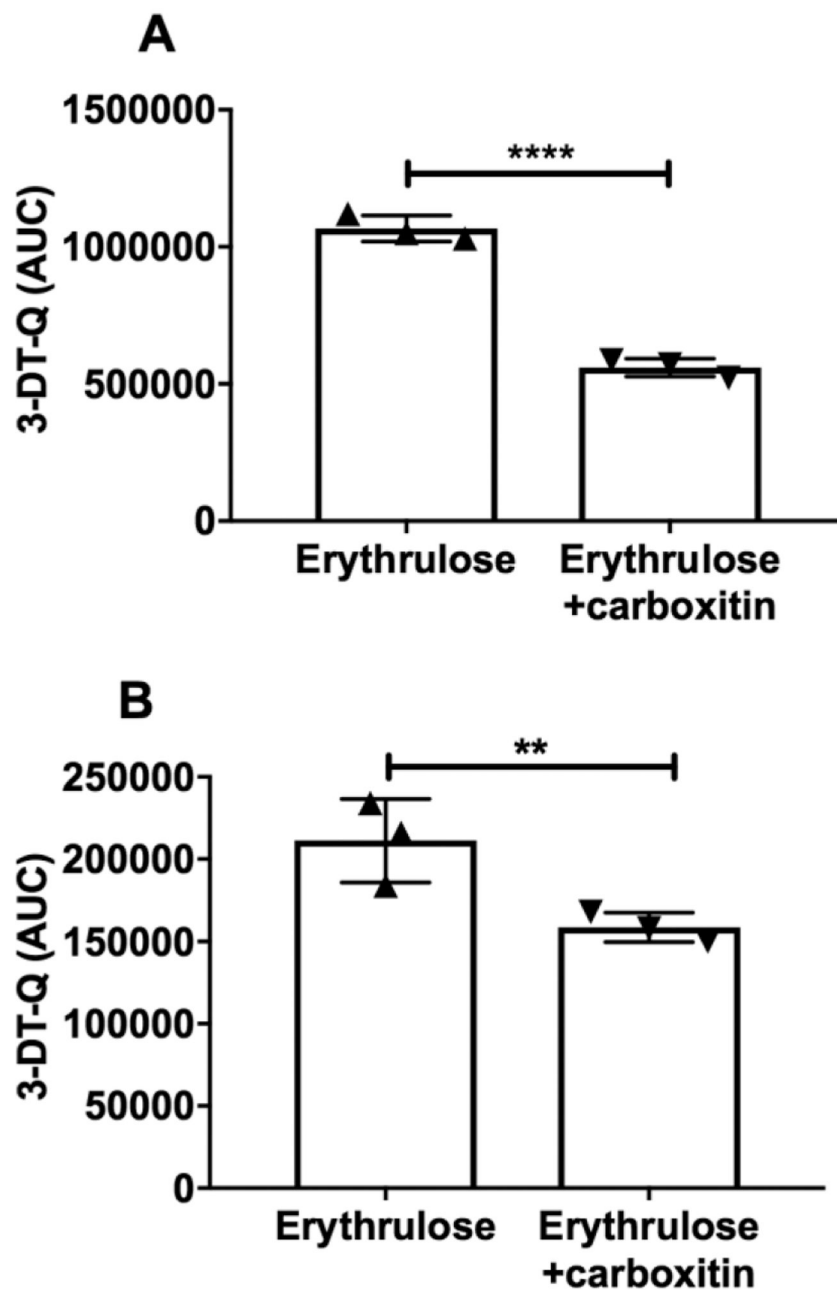


Fig. 6. Carboxitin traps a dicarbonyl formed from erythulose degradation.

(A) Carboxitin (1 mM) was coincubated with erythulose (1 mM) for 3 days at 37°C in 40 mM HEPES, pH 7. (B) Erythulose (30 mM) was first incubated alone for 2 days under similar conditions, after which the erythulose was diluted to 1 mM and coincubated with 1 mM carboxitin for another 1 day under similar conditions. Both incubation mixtures were then OPD derivatized for another 6 h at room temperature and analyzed for the quinoxaline derivative 3-DT by UPLC-MS². Bar graphs represent the means \pm SD of triplicate measurements. ** $p < 0.01$; **** $p < 0.0001$.

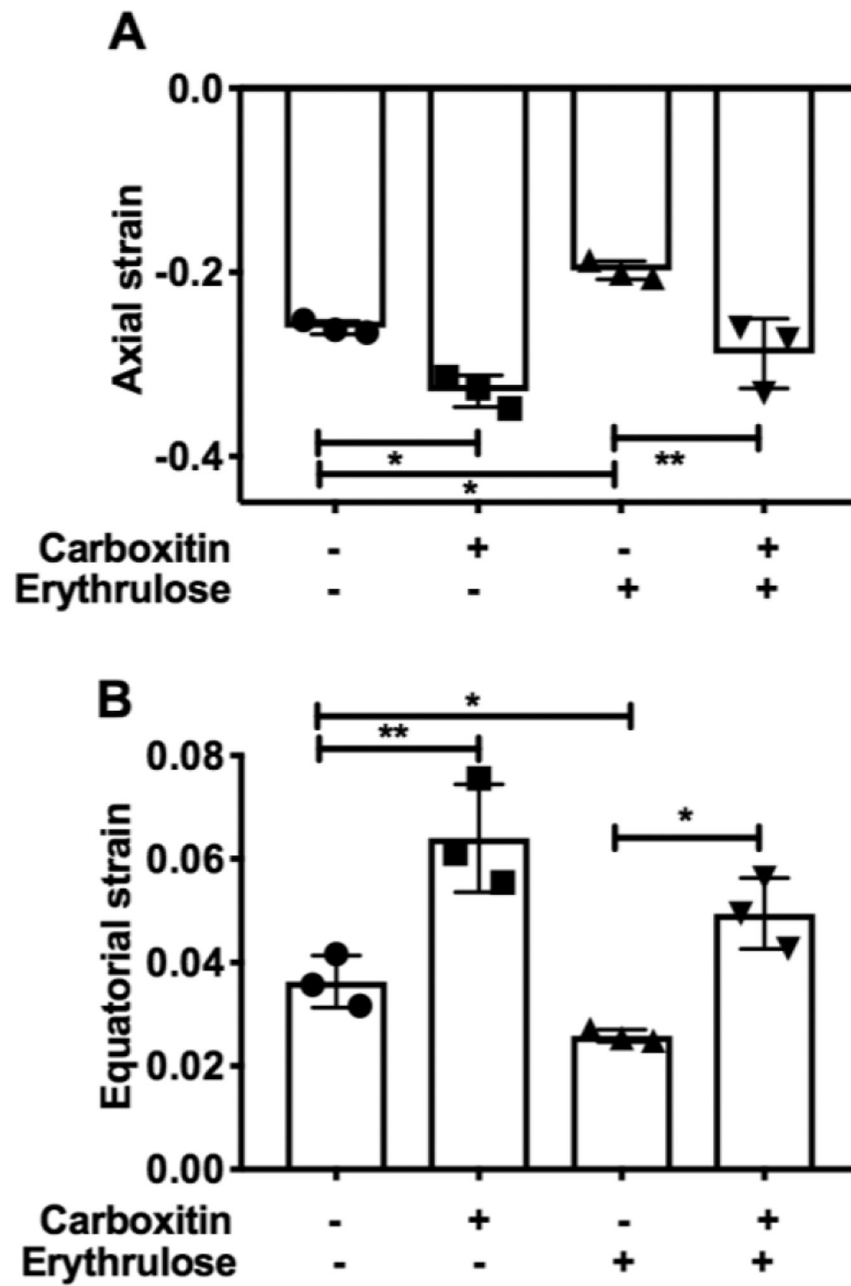


Fig. 7. Carboxitin decreases the stiffness of mouse lenses. Compressive strain along the (A) axial and (B) equatorial regions is plotted for mouse lenses treated with or without carboxitin against a fixed applied load. Bar graphs represent the means \pm SD of triplicate measurements. * $p < 0.05$; ** $p < 0.01$.

Table 1.

Mass spectrometric parameters for estimation of carboxitin and its degradation products.

	Qualifier 1					Qualifier 2					
	Q1 [m/z]	DP [V]	Q3 [m/z]	CE [eV]	CXP [V]	Q3 [m/z]	CE [eV]	CXP [V]	Q3 [m/z]	CE [eV]	CXP [V]
Carboxitin	481.2	41	117.9	57	8	152.0	32	10	205.1	35	15
Carboxitin - 1*EtOH	453.1	40	324.1	26	7	152.0	31	10	118.0	35	7
Carboxitin - 2*EtOH	425.1	35	296.1	24	13	152.0	31	8	118.0	31	10
GSH-NEM	433.0	40	304.0	20	12	201.0	29	14	287.0	30	15
MEG-NEM	244.9	35	186.0	26	12	125.9	34	8	143.9	47	10
GSH-OEt ₂ -NEM	489.2	35	332.2	21	8	200.9	34	10	314.9	29	11
GSH-OEt-NEM (1)	461.2	45	304.2	25	20	287.1	30	10	201.1	32	10
GSH-OEt-NEM (2)	461.2	45	332.2	22	15	201.1	32	10	212.1	37	15

Table 2.

Mass spectrometric parameters for estimation of AGEs.

AGE	Quantifier					Qualifier 1					Qualifier 2						
	Q1 [m/z]	DP (V)	Q3 [m/z]	CE [eV]	CXP [V]	Q3 [m/z]	CE [eV]	CXP [V]	Q3 [m/z]	CE [eV]	CXP [V]	Q3 [m/z]	CE [eV]	CXP [V]	Q3 [m/z]	CE [eV]	CXP [V]
CML	205.1	40	130.2	17	11	84.1	25	13	56.1	50	10	56.1	59	8	56.1	32	9
CEL	219.1	54	84.1	33	11	130.1	18	12	130.2	25	10	130.1	26	11	169.1	29	11
GOLA	333.2	40	84.3	54	11	169.1	26	12	198.1	45	14	267.3	45	15	197.4	45	14
GOLD	327.2	60	84.1	55	13	282.3	29	11	198.1	25	19	198.1	25	19	198.1	25	19
MODIC	357.3	25	312.2	31	14	267.3	45	15	197.4	45	14	197.4	45	14	197.4	45	14